POLARIZATION MEASUREMENT OF GRB 041219A WITH SPI

E. Kalemci[1], **S. E. Boggs**[2], **C. Kouveliotou**[3], **M. Finger**[3], and **M. G. Baring**[4]

[1]*Sabancı Universitesi, Orhanlı-Tuzla, İstanbul, 34956, Turkey.*
[2]*Space Sciences Laboratory, 7 Gauss Way, University of California, Berkeley, CA, 94720-7450, USA.*
[3]*NASA Marshall Space Flight Center, SD-50, Huntsville, AL, 35812, USA.*
[4]*Department of Physics and Astronomy, MS-108, Rice University, P.O. Box 1892, Houston, TX 77251*

ABSTRACT

Measuring the polarization of the prompt γ-ray emission from GRBs can significantly improve our understanding of both the GRB emission mechanisms, as well as of the underlying engine driving the explosion. We searched for polarization in the prompt γ-ray emission of GRB 041219a with the SPI instrument. Using multiple-detector coincidence events in the 100–350 keV energy band, our analysis yields a polarization fraction from this GRB of $98 \pm 33\%$. Statistically, we cannot claim a polarization detection from this source. We cannot strongly rule out the possibility that the measured modulation is dominated by instrumental systematics. Therefore, SPI observations of GRB 041219a do not significantly constrain GRB models. However, this measurement demonstrates the capability of SPI to measure polarization, and the techniques developed for this analysis.

Key words: polarization, techniques: polarimetric, gamma rays: bursts.

1. INTRODUCTION

Despite the extensive work in recent years on GRB afterglows, the nature of the central driver that powers the burst and the prompt γ-ray emission mechanism remain enigmatic. In the models invoking merging neutron stars and 'collapsars', hydrodynamically dominated outflows (jets) transport the bulk GRB kinetic energy. Alternatively, Poynting-flux may be the driver for the transport of energy to large distances. Synchrotron radiation has traditionally been the favored emission mechanism of the prompt γ-ray emission though competing Compton upscatering and synchrotron-self Compton models have been put forward [reviews of GRB models can be found in 1, 2]. In terms of polarization modeling, synchrotron radiation is naturally a strong candidate [3], but a portion of the polarized photon signal may also be Compton up-scattered [4]. A definite measurement of polarization properties from the prompt emission of GRBs will probe their anisotropy or magnetic field geometry, and thereby help determine the nature of the central engine and the γ-ray emission mechanism.

The first detection of the linear polarization from the prompt γ-ray emission of a GRB with the *RHESSI* instrument indicated a polarization fraction of 80 ± 20 % [5]. However, independent analyses of the *RHESSI* data by other groups were not able to confirm this result at the same level of significance [6]. Clearly, more measurements, using different instruments and techniques, are required [7].

In this letter, we discuss methods to measure polarization using SPI, and apply these methods to measure the polarization properties of the bright and long GRB 041219a. The details of the analysis can be found in [8]. The burst is in the fully coded field of view of both the ISGRI and the SPI, and is $\sim 3°$ off the X-axis. The brightest part of the burst saturated the available telemetry of *INTEGRAL*. A comprehensive spectral and temporal analysis of the burst with SPI, *SWIFT*-BAT, and the *RXTE* ASM is given in [9].

2. ANALYSIS

2.1. SPI and γ-ray polarization

The events that are singly scattered from one detector and photo-absorbed in a second separate detector (multiple events, ME) are sensitive to the incident γ-ray polarization since linearly polarized gamma-rays preferentially scatter in azimuthal directions perpendicular to their electric polarization vector.

The two main parameters that determine the sensitivity of a multi-detector instrument to gamma-ray polarization are the effective area to the multiple-detector scatter events, and the average value of the polarimetric modulation factor Q, which is the maximum variation in the azimuthal scattering probability for polarized photons [10, 11]. For a source count rate of S, and fractional polarization of Π_s, the expected azimuthal scattering angle

(ϕ) distribution is

$$\frac{dS}{d\phi} = \frac{S}{2\pi}[1 - Q\,\Pi_s \cos 2(\phi - \eta)]. \quad (1)$$

Therefore, the "signature" of polarization is a 180°-periodic modulation in the distribution of azimuthal scattering angles, with a minimum at the polarization angle η.

2.2. GRB 041219a SPI data

The SPI light curve indicates that the GRB were affected by the telemetry saturation problems which also affected the IBIS data [12]. The 100-500 keV (total energy) light curve of ME, corrected for effective dead-time due to the missing packets, is shown in Fig. 1. Characterizing this effective dead-time is important in terms of determining the correct background rate for the regions with the packet loss problem.
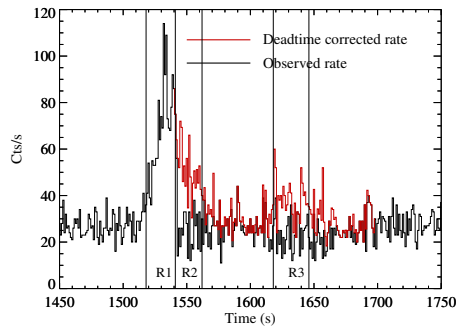

Figure 1. The observed (black histogram) and the reconstructed (red histogram) light curve of ME events in 100–500 keV band. The gaps are treated as dead-time. The vertical solid lines separate R1, R2, R3 regions (see text).

2.3. MGEANT simulations

To determine the polarization fraction for this GRB, we need to compare the measured azimuthal scattering angle distribution to the expected distribution for an unpolarized and a polarized source from this sky location. The only method available for performing this comparison is with detailed Monte-Carlo simulations. The response to a polarized source is characterized by the polarimetric modulation factor, Q, discussed in § 2.1. Since Q is energy-dependent, it will depend on the energy spectrum of the source. The simulations are performed using MGEANT, which is a γ-ray instrument simulation package developed at NASA/GSFC. More information on MGEANT and the complete mass model we used can be found in [13].

2.4. GRB 041219a spectrum

Detailed and precise determination of the GRB 041219a spectral parameters is not necessary for this work as Q is not strongly dependent on the exact spectral parameters. To determine the spectral parameters, we first obtained the singles count spectrum. For background, we took the data from the first 1000 s from the beginning and applied two corrections to take into account evolution and dead-time. An example spectrum after background subtraction is shown in Fig. 2.
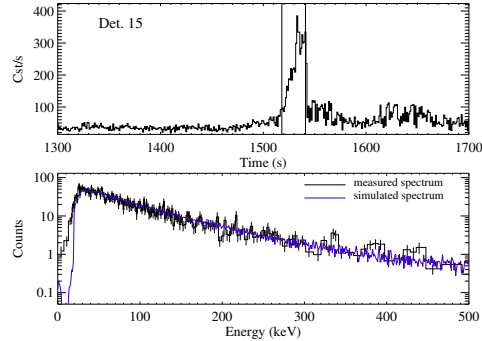

Figure 2. The top panel shows the singles light curve of Detector 15 in 30–490 keV band. No dead-time correction is applied. The solid vertical lines indicate the region (R1) for which the spectrum is extracted. The bottom panel shows the measured (black histogram), and the simulated (purple) spectrum.

After the photons from the GRB event were isolated and spectra for each detector were obtained, the next step is to reproduce these spectra with simulations. We ran three simulations with the Band Function [14] spectrum using (1) α=1.0, β=2.4, E_{br}=170, (2) α=1.0, β=2.0, E_{br}=170, and (3) α=1.0, β=2.0, E_{br}=200.

We applied all the corrections to the simulated data as described in [13]. We also applied a correction for dead-time for each detector. We found that the spectrum with these set of parameters, α=1.0, β=2.0, E_{br}=200, best describes the data in R1. In Fig. 2, we show the actual and the simulated spectrum of Detector 15 as an example.

2.5. Modulation Factor

The next step to measure polarization is to obtain Q by comparing the azimuthal scattering angle distributions of non-polarized and 100% polarized photons. For the spectrum of GRB 041219a, most of the photons Compton scattered from the low energy deposition detector to the high energy deposition. Therefore, for the actual data we tag the direction of every photon as originating from the center of the lower energy deposition detector to the center of the higher energy deposition detector. The final results should not be affected by the incorrectly tagged events due to the 180° symmetry of the polarization modulations.
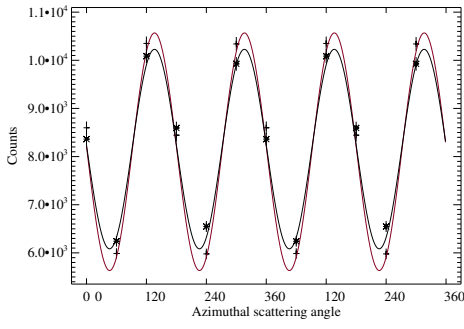
Figure 3. Simulated azimuthal scattering angle distribution of 100% polarized photons at 200 keV originating at the GRB position. Black fit: pixellated, Red fit: interaction positions within the detectors
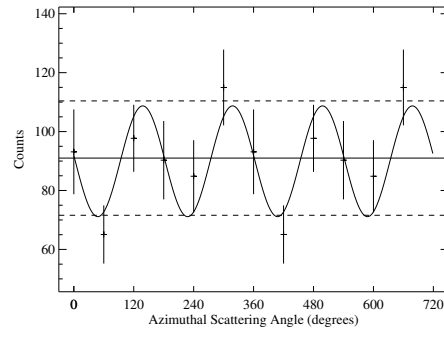

Figure 4. The azimuthal scattering angle distribution of events in Region 1, and a $\cos 2(\phi - \eta)$ fit to the data. The solid line is the average (no polarization) and the dashed lines show the maximum and the minimum modulation for a 100% polarization fraction.

On the other hand, MGEANT simulations provide more information than that of the real data. First, in simulations, the interaction positions within the individual detectors are known. Second, for any incoming photon energy, the direction of the photon is also known. We determined azimuthal scattering angle distributions for three cases; (a) using the actual interaction positions and directions determined by the simulation, (b) using the detector center-center angles (pixellation) and directions determined by the simulation, (c) using the center-center angles and directions determined using energy depositions. Cases (a) and (b) can only be calculated using the simulations, and (c) represents the distribution for the actual data.

We obtained the modulation factors by following the method described in [11]. For the simulated events with 100% polarized photons (Π_s=1) the modulation factor can be obtained by fitting the azimuthal scattering angle distribution with a $\cos 2(\phi - \eta)$ function (see Eq. 1). However, before doing this, one needs to take into account the "response" of the distribution for non-polarized photons. This response is obtained by dividing the non-polarized simulated azimuthal scattering angle distribution by its average.

Fig. 3 shows the azimuthal scattering angle distribution of 100% polarized photons at 200 keV as an example. The amplitude of the modulation with respect to the average gives the modulation factor. The pixellation reduces the modulation factor around 20% (with respect to non-pixellated modulation) at 200 keV.

We ran more simulations with mono-energetic photons at different energies, with non-polarized and 100% polarized photon and confirmed that the ~3° off-axis position of the GRB, and the reduced number of detectors did not affect the modulation factors significantly. More importantly, using the energy depositions to determine the directions rather than using the actual directions has no effect on the modulation factor.

Finally, by using simulations with the GRB spectrum de-

scribed above, we determined the modulation factor for R1 in 100–350 keV band.

3. POLARIZATION MEASUREMENT

We applied these cuts to the ME: The minimum allowed energy for each detector in a pair is 26 keV, the minimum allowed total energy of a pair is 100 keV, and the maximum allowed total energy of a pair is 350 keV. The minimum cuts are necessary to ensure that the events are actual Compton events. Due to low count rates and low modulation factors, including the very high energy part does not improve the measurement. To obtain maximum allowed total energy we considered the signal/noise ratio of MEs for different energies, their respective modulation factors, and finally the fraction of the incorrectly tagged events. And finally, we cut all MEs with total energies between 184 keV and 201 keV to remove significant number of background photons in the prominent Ge line at 198 keV.

We separated the light curve in three regions. Region 1 is from the beginning of the burst to time that the packet-loss problems began. Region 2 and Region 3 are determined using the source and background rates to maximize the source to background ratio. These regions are denoted as R1, R2, and R3 in Fig. 1. For R1, the total number of source counts is 543, and the total number of background counts is 173.

The simulated, non-polarized events are corrected for mass and dead-time. After these corrections, we histogrammed the simulated data exactly as we histogrammed the real data. To obtain the polarization fraction, we followed the method described in Section 2.3. The resultant distribution and the $\cos 2(\phi - \eta)$ fit is shown in Fig. 4. The best fit modulation amplitude is $Q\Pi_s$ =20.8 ± 7.8%, corresponding to a polarization angle η = 48.3° ± 3.8°. The χ^2 for this best fit is 2.61 for 3 degrees of freedom (DOF). For comparison, the χ^2 for
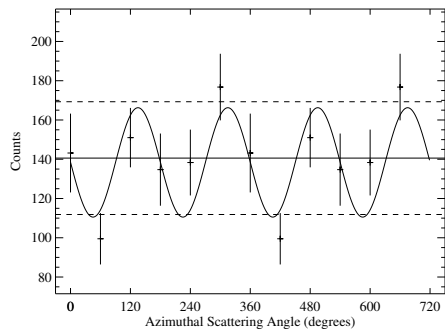
Figure 5. The azimuthal scattering angle distribution of events in Regions 1, 2 and 3 and a $\cos 2(\phi - \eta)$ fit to the data. The solid line is the average (no polarization) and the dashed lines show the maximum and the minimum modulation for a 100% polarization fraction.

the best fit assuming no polarization (flat distribution) is 11.00 for 5 DOF. For polarization angles $\eta \sim 45°$, we calculate that the polarimetric modulation factor, Q=21.2. Correcting the best fit modulation amplitude for this factor yields a best fit polarization amplitude of $\Pi_s = 98 \pm 38\%$, providing no upper bound.

For the combined case (R1+R2+R3), the source counts and background counts are 839 and 389 respectively. Because of the evolution of the GRB spectra, the combined spectrum is slightly softer than the spectrum of R1. We determined that a Band function with α=1.15, β=2.4, E_{br}=180 fits the overall spectrum well.

The azimuthal scattering angle distribution for the combined case is shown in Fig. 5. The fit shown yields a modulation amplitude of $Q\Pi_s$=19.9$\pm$6.7% with a minimum at 45.8° $\pm$ 5.2°. The modulation factor at this angle is 20.4%, corresponding to $\Pi_s = 98 \pm 33\%$. The χ^2 for the $\cos 2(\phi - \eta)$ fit is 4.71 for 3 degrees of freedom (DOF), whereas the χ^2 for the flat distribution is 15.03 for 5 DOF. Neither of these fits represent the data well, as seen in Fig. 5, and also inferred from the χ^2 values. Given our measurement uncertainties, and assuming an unpolarized (flat) distribution, a simple Monte-Carlo simulation yields the chance probability of fitting a modulation of this amplitude as 1.01 %. The best-fit polarization yields a lower reduced χ^2 over the fit assuming no polarization, with an F-test [15] value of 3.29.

4. DISCUSSION

We have demonstrated techniques to measure polarization of the prompt γ-ray emission of a GRB in the field-of-view of SPI on *INTEGRAL*. However, for GRB 041219a, we have not strongly constrained models for the emission mechanism nor the central engine. There simply is not enough ME for statistically significant measurements

The quoted numbers in this work are for the cases with the largest polarization fractions with the highest F-test values compared to a flat distribution. However, choosing different energy bands for minimum and maximum energies yields lower polarization fractions. We obtain significantly lower polarization fractions if the 198 keV Ge line is not filtered out. The polarization angle may be changing with energy, causing a decrease in the overall modulation. Unfortunately the statistics are not good enough to test this hypothesis.

Our analysis indicates that systematic effects from the two inactive SPI detectors, as determined from pre-flight calibration data, should not significantly affect these polarization measurements.

REFERENCES

[1] Piran, T. 1999, Physics Reports, 314, 575

[2] Mészáros, P. 2001, Science, 291, 79

[3] Granot, J. 2003, ApJ, 596, L17

[4] Eichler, D. & Levinson, A. 2003, ApJ, 596, L147

[5] Coburn, W. & Boggs, S. E. 2003, Nature, 423, 415

[6] Wigger, C., Hajdas, W., Arzner, K., Güdel, M., & Zehnder, A. 2004, ApJ, 613, 1088

[7] Willis, D. R., Barlow, E. J., Bird, A. J., et al. 2005, A&A, 439, 245

[8] Kalemci, E., Boggs, S. E., Kouveliotou, C., et al. 2007, ApJS, accepted, astro-ph/0610771

[9] McBreen, S., Hanlon, L., McGlynn, S., et al. 2006, A&A, 455, 433

[10] Novick, R. 1975, Space Science Reviews, 18, 389

[11] Lei, F., Dean, A. J., & Hills, G. L. 1997, Space Science Reviews, 82, 309

[12] Gotz, D., Mereghetti, S., Shaw, S., Beck, M., & Borkowski, J. 2004, GRB Circular Network, 2866

[13] Sturner, S. J., Shrader, C. R., Weidenspointner, G., et al. 2003, A&A, 411, L81

[14] Band, D., Matteson, J., Ford, L., et al. 1993, ApJ, 413, 281

[15] Bevington, P. R. & Robinson, D. K. 1992, Data reduction and error analysis for the physical sciences (New York: McGraw-Hill, —c1992, 2nd ed.)